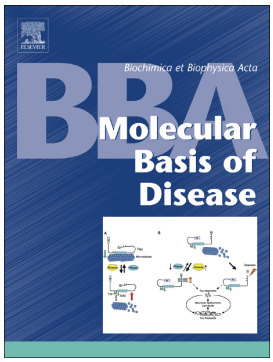

Empagliflozin improves left ventricular diastolic function of db/db mice

Julia Moellmann, Barbara M. Klinkhammer, Patrick Droste, Ben Kappel, Elias Haj-Yehia, Sebastian Maxeiner, Anna Artati, Jerzy Adamski, Peter Boor, Katharina Schütt, Gary D. Lopaschuk, Subodh Verma, Nikolaus Marx, Michael Lehrke

PII: S0925-4439(20)30152-6

DOI: https://doi.org/10.1016/j.bbadis.2020.165807

Reference: BBADIS 165807

To appear in: *BBA - Molecular Basis of Disease*

Received date: 19 December 2019

Revised date: 9 April 2020

Accepted date: 15 April 2020

Please cite this article as: J. Moellmann, B.M. Klinkhammer, P. Droste, et al., Empagliflozin improves left ventricular diastolic function of db/db mice, *BBA - Molecular Basis of Disease* (2020), https://doi.org/10.1016/j.bbadis.2020.165807

Empagliflozin improves left ventricular diastolic function of db/db mice

Julia Moellmann[1], Barbara M. Klinkhammer[2], Patrick Droste[2], Ben Kappel[1], Elias Haj-Yehia[1], Sebastian Maxeiner[1], Anna Artati[3], Jerzy Adamski[3, 6, 7, 8], Peter Boor[2], Katharina Schütt[1], Gary D. Lopaschuk[4], Subodh Verma[5], Nikolaus Marx[1§], Michael Lehrke[1§]

[1]Department of Internal Medicine I; University Hospital Aachen, RWTH Aachen University, Aachen, Germany; [2]Institute of Pathology, University Hospital Aachen, RWTH Aachen University, Aachen, Germany; [3]Research Unit Molecular Endocrinology and Metabolism, Helmholtz Centrum Munich, German Research Center for Environmental Health (GmbH), Munich-Neuherberg, Germany; [4]Cardiovascular Research Centre, University of Alberta, Edmonton, Alberta, Canada; [5]Division of Cardiac Surgery, Keenan Research Centre for Biomedical Science and Li Ka Shing Knowledge Institute of St. Michael's Hospital, Toronto, ON, Canada; [6]Chair of Experimental Genetics, Technical University of Munich, Freising-Weihenstephan, Germany; [7]German Center for Diabetes Research (DZD e.V.), Munich-Neuherberg, Germany; [8]Department of Biochemistry, Yong Loo Lin School of Medicine, National University of Singapore, Singapore

§ Corresponding authors:
Michael Lehrke MD & Nikolaus Marx, MD, FESC, FAHA
Department of Internal Medicine I
University Hospital Aachen, RWTH Aachen University
Pauwelsstraße 30
D-52074 Aachen
Germany
Phone: +49 241 80-89300
Fax: +49 241 80-82545
E-mail: mlehrke@ukaachen or nmarx@ukaachen.de

Total word count: 4242

Key words: empagliflozin, SGTL2 inhibitors, cardiovascular disease, type 2 diabetes mellitus, branched-chain amino acids, ketone bodies

Abstract:

Objectives: Investigation of the effect of SGLT2-inhibition by empagliflozin on left ventricular function in a model of diabetic cardiomyopathy.

Background: SGLT2 inhibition is a new strategy to treat diabetes. In the EMPAREG Outcome trial empagliflozin treatment reduced cardiovascular and overall mortality in patients with diabetes presumably due to beneficial cardiac effects, leading to reduced heart failure hospitalization. The relevant mechanisms remain currently elusive but might be mediated by a shift in cardiac substrate utilization leading to improved energetic supply to the heart.

Methods: We used db/db mice on high-fat western diet with or without empagliflozin treatment as a model of severe diabetes. Left ventricular function was assessed by pressure catheter with or without dobutamine stress.

Results: Treatment with empagliflozin significantly increased glycosuria, improved glucose metabolism, ameliorated left ventricular diastolic function and reduced mortality of mice. This was associated with reduced cardiac glucose concentrations and decreased calcium/calmodulin-dependent protein kinase (CaMKII) activation with subsequent less phosphorylation of the ryanodine receptor (RyR). No change of cardiac ketone bodies or branched-chain amino acid (BCAA) metabolites in serum were detected nor was cardiac expression of relevant catabolic enzymes for these substrates affected.

Conclusions: In a murine model of severe diabetes empagliflozin-dependent SGLT2 inhibition improved diastolic function and reduced mortality. Improvement of diastolic function was likely mediated by reduced spontaneous diastolic sarcoplasmic reticulum (SR) calcium release but independent of changes in cardiac ketone and BCAA metabolism.

1. Introduction

Inhibition of the sodium-dependent glucose transporter 2 (SGLT2) is a pharmacological approach to treat diabetes by increasing urinary glucose excretion, thus reducing blood glucose levels. Importantly, in three large cardiovascular outcome trials (CVOTs) (EMPA-REG Outcome (empagliflozin), CANVAS (canagliflozin) and DECLARE (dapagliflozin)), SGLT2 inhibitors reduced heart failure events in high-risk type 2 diabetes patients. Besides, SGLT2 inhibition reduced heart failure hospitalization and cardiovascular death in patients with preexisting heart failure (HFrEF) with and without diabetes. Separation of event curves occurred early within the trials demonstrating immediate effectiveness of the drugs [1-3].

Various mechanisms have been discussed to explain this beneficial finding including hemodynamic effects, effects on blood pressure and arterial stiffness, as well as changes in cardiac energy metabolism and substrate utilization [4]. Urinary glucose excretion caused by SGLT2 inhibition has been hypothesized to shift cardiac substrate utilization to a preferred utilization of ketone bodies, fatty acids and BCAAs mimicking a fasting response [5-8]. Data from our group, employing an unbiased metabolomic approach in empagliflozin-treated patients with type 2 diabetes and cardiovascular (CV) disease, suggest that SGLT2 inhibitor treatment leads to an expanded ketone body utilization and an increased BCAA catabolism [9]. Since ketone utilization is increased in advanced heart failure, enhanced ketone body catabolism mediated by empagliflozin may be beneficial and potentially contribute to the reduction in heart failure hospitalization seen in the CVOTs mentioned above [10, 11].

In the present study, we investigated effects of SGLT2 inhibition on cardiac function and metabolism in the murine diabetes model of db/db mice on a high fat western-type diet.

2. Methods

2.1. Animal studies

All experiments were approved by the government of North Rhine-Westphalia (Germany). Male db/db and adequate control mice (db/db: BKS(D)-Lepr$^{db/db}$/JOrlRj

and control: BKS(D)-Lepr$^{db/+}$/JOrlRj), 6 weeks of age were obtained from Janvier Labs and placed in a 12 h day-night cycle with unlimited supply of food and water in the animal facility of the University Hospital of the RWTH Aachen University. After a one-week adaptation to our facility, mice were fed a high fat western-type diet (39 kJ% fat, 41 kJ% carbohydrates and 20 kJ% protein; ssniff EF R/M acc. TD88137AQ8 mod.; ssniff Spezialdiäten GmbH) for 4.5 weeks with or without empagliflozin in a concentration of 150 mg/kg. Urine collection was performed in metabolic cages for 16 hours with an unlimited supply of water and urinary glucose concentration was assessed by the chemistry department of the animal facility of the University Hospital RWTH Aachen. Hemodynamics were measured by Millar catheter (Millar Instruments) after advancing the catheter across the right carotid artery through the aortic valve into the left ventricle of anesthetized mice. Basal measurement was followed by i.p. injection of dobutamine (5 µl/g body weight) as a cardiac stress test. Signals were continuously recorded and analyzed using iox (emka Technologies). Finally, overnight fasted mice were sacrificed by cervical dislocation, blood glucose levels were assessed using a glucometer (Contour, Bayer) and tissue samples were snap-frozen in liquid nitrogen and stored at −80°C for further analysis.

2.2. Blood sample analysis

Serum concentrations of B-type natriuretic peptide (BNP) (Cloud-Clone Corp.) were determined by enzyme-linked immunosorbent assay (ELISA) according to the manufacturer's protocol. Serum cholesterol (CHOL) and triglycerides (TG) (both Diasys Diagnostics) were measured enzymatically by CHOD-PAP method using commercial reagents for photometric systems (Tecan).

2.3. Gene expression analysis by RT-PCR

Total ribonucleic acid (RNA) was isolated with the RNeasy Mini Kit (heart and liver) and RNA preparation was followed by DNase digestion and reverse transcription into complementary DNA (cDNA) (Invitrogen). Gene expression was quantified by the use of SYBR reagents with a ViiATM 7 Real-Time PCR System (Applied Biosystems). Measurements were conducted in duplicates under standard reaction conditions and normalized to *Actb* (β-actin). Genes were selected concerning their pathophysiological/physiological function (heart failure: *Anp*; mitochondrial transcription factors: *Pgc-1α*, *Tfam*; mitochondrial fusion (*Mfn-2*, *Opa-1*) and fission (*Drp-1*, *Fis-1*); BCAA catabolism: *Bckde2*, *Bckd kinase*, *Bcat2*, *Bckde1b*, *Ppm1k*;

inflammation: *Il-1β*, *Il-6*, *Tnfα*, *Infγ*, *F4/80*, *Ccl2*). Primers were obtained from Eurofins Genomics and all primer sequences are presented in supplementary table 1.

2.5. Western Blot analysis

Heart tissue samples were homogenized in lysis buffer (0.25 M Sucrose, 2.2 mM Na2-EDTA, 10 mM Tris and complimented with PhosSTOP and cOmplete from Roche), then separated on a 4-15% gradient SDS-gel and transferred to a nitrocellulose membrane. All antibodies were obtained from Cell Signaling if not indicated otherwise: AKT1, phospho-AKT (Thr308), AMPKα, phospho-AMPKα (Thr172), phospho-CaMKII (Thr286), CaMKII, GLUT4, GAPDH, phospho-Troponin I (cardiac) (Ser23/24) (all concentration 1:1.000), BDH-1 (concentration 1:500) (Thermo Fisher), OXCT1 (SCOT) (concentration 1:500) (Sigma-Aldrich/Merck), phospho-BCKDHA (Ser293), BCKDHA, DBT, OXPHOS, ryanodine receptor 2/RYR-2 and phosphor-ryanodine receptor 2/RYR-2 (Ser2808) (all concentration 1:500) (abcam) and ANP, PGC1α and SERCA2 (concentration 1:1.000) (Santa Cruz) and anti-rabbit or anti-mouse IgG, HRP-linked antibodies were used as secondary antibody (both concentration 1:1.000). Western blots were detected by Chemi DocTM MP Imaging System (BioRad) and analyzed with the software Image Lab 5.0 (BioRad).

2.6. Histological analysis

Heart tissue was fixed in 4% paraformaldehyde overnight and embedded in paraffin. The heart was cut in direction from top to apex and 4 µm sections were collected after the mitral valve. Collagen was visualized by Gomori's one-step trichrome stain and analyzed with the software Image-Pro Plus 7.0 (Media Cybernetics).

To analyze the size and area of cardiomyocytes tissue sections were rehydrated and heat-induced antigen retrieval was performed in citrate buffer. Slides were incubated with fluoresein-coupled WGA (wheat germ agglutinin, 1:100 (Vector Laboratories)) and counterstained with DAPI. Slides were digitalized using Aperio Versa200 whole slide scanner (Leica Biosystems). In each mouse 150-200 cross-cut cardiomyocytes were measured and analyzed using ImageJ (NIH).

2.7. Metabolomics analysis

Untargeted metabolomics analysis was performed at the Genome Analysis Center, Research Unit Molecular Endocrinology and Metabolism, Helmholtz Centrum Munich. Frozen mice cardiac samples were weighted and were placed into pre-cooled (dry ice) 2 ml homogenization tubes containing ceramic beads with a diameter of 1.4 mm (Precellys® Keramik-Kit 1.4 mm). Pre-cooled water in a ratio of 5 µl/mg tissue was added into the tubes. The samples were then homogenized in a Precellys 24 homogenizer (PEQLAB Biotechnology GmbH) equipped with an integrated cooling unit for 3 times 20 s at 5,500 rpm, with 30 s intervals (to ensure freezing temperatures in sample vials) between the homogenization steps. Hundred µl of the cardiac homogenate was loaded onto a 2 ml 96- deep well plate. In a separate sample set, 100 µl mice plasma samples were loaded onto a separate 2 ml 96- deep well plate. Three types of quality control samples were analyzed in concert with the experimental samples in each sample set: samples generated from a pool of human plasma; samples generated from a small portion of each sample of the study served as technical replicate throughout the data set; and extracted water samples served as process blanks. Experimental samples and controls were randomized across the platform run.

The 100 µl of the sample in each well of the 2 ml 96- deep well plate were extracted with 500 µl methanol, containing four recovery standards to monitor the extraction efficiency. After centrifugation, the supernatant was split into 4 aliquots into two 96-well microplates. The first 2 aliquots were used for ultra-high performance liquid chromatography-tandem mass spectrometry (UPLC-MS/MS) analysis in positive and negative electrospray ionization mode. Two further aliquots on the second plate were kept as backup. The extract aliquots were dried on a TurboVap 96 (Zymark).

Before UPLC-MS/MS analysis, the dried extract samples were reconstituted in acidic or basic LC-compatible solvents, each of which contained 8 or more standard compounds at fixed concentrations to ensure injection and chromatographic consistency. The UPLC-MS/MS platform utilized a Waters Acquity UPLC with Waters UPLC BEH C18-2.1×100 mm, 1.7 µm columns and a Thermo Scientific Q-Exactive high resolution/accurate mass spectrometer interfaced with a heated electrospray ionization (HESI-II) source and Orbitrap mass analyzer operated at 35,000 mass resolution. Extracts reconstituted in acidic conditions were gradient eluted using water and methanol containing 0.1% formic acid, while the basic

extracts, which also used water/methanol, contained 6.5mM ammonium bicarbonate. The MS analysis alternated between MS and data-dependent MS2 scans using dynamic exclusion, and the scan range was from 80-1000 m/z.

Metabolites were identified by automated comparison of the ion features in the experimental samples to a reference library of chemical standard entries that included retention time, molecular weight (m/z), preferred adducts, and in-source fragments as well as associated MS spectra and curated by visual inspection for quality control using software developed at Metabolon (Metabolon, Inc.). Chromatographic peaks were quantified using area-under-the-curve. Metabolomics data were analyzed by 1-way ANOVA using GraphPad PRISM (GraphPad Software, Inc.).

3. Results

In our model of db/db mice on high-fat diet (HFD) empagliflozin treatment for 4.5 weeks increased glucosuria (Figure 1a) and reduced blood glucose levels (Figure 1b) but did not affect body weight (Figure 1c). This was accompanied by a significant reduction of serum cholesterol but no effect on triglycerides (Figure 1d). Liver weight (Figure 1e) was significantly reduced by empagliflozin without a difference in hepatic lipid content (Figure 1f). Hepatic inflammatory cytokine expression was significantly increased in the diabetic milieu of db/db mice and significantly reduced by empagliflozin treatment (Figure 1g and h). Interestingly, empagliflozin led to a robust reduction of mortality (Figure 1i) of severely diabetic db/db mice: after 4.5 weeks 54% of db/db mice on HFD died while all heterogeneous wild type as well as all empagliflozin-treated db/db mice on HFD were alive.

To investigate whether the reduction in mortality was attributable to improved cardiac function we assessed cardiac contractility by Millar catheter with and without dobutamine stress. Empagliflozin significantly improved cardiac relaxation as an indicator of diastolic function while affecting systolic left ventricular function by trend and showed no effect on heart rate (Figure 2a-c). No significant difference in heart weight (Figure 2d) and BNP concentrations (Figure 2e) nor cardiac atrial natriuretic peptide (ANP) protein nor mRNA expression (Figure 2f-h) were detected between empagliflozin and control-treated db/db mice. Furthermore, no significant differences

in cardiac morphology measured by fibrosis (Figure 2i and j) and left ventricular wall thickness (Figure 2k) nor cardiomyocyte diameter or area (Figure 2i, l and m) were found between groups.

Given that changes in cardiac energy substrate utilization have been discussed to contribute to the beneficial effects seen on heart failure hospitalization in SGLT2 inhibitor-treated patients, we next analyzed the expression of enzymes relevant for cardiac energy substrate metabolism in our model. First, we analyzed cardiac glucose metabolism and found an increase in AKT(Thr308)-phosphorylation by empagliflozin treatment suggesting improved cardiac insulin signaling (Figure 3a and b). In contrast, empagliflozin did not affect the expression of cardiac glucose transporter GLUT4 (Figure 3a and b). Further, we found no changes for sarcoplasmic/endoplasmic reticulum calcium ATPase (SERCA) (Figure 3a and c) while AMPK(Thr172)-phosphorylation as an indicator of energy metabolism (Figure 3a and c) was slightly increased. Next, we assessed PGC1α, *Tfam*, and OXPHOS as regulators and effectors of mitochondrial function in addition to genes relevant for mitochondrial fusion and fission without finding differences between groups (Figure 3d-h). To evaluate changes in cardiac energy substrate metabolism as a possible cause for the beneficial effects of empagliflozin treatment, we analyzed beta-hydroxybutyrate dehydrogenase (BDH-1), a key enzymes of ketone body catabolism, which was significantly reduced in db/db mice relative to wild type controls but not affected by empagliflozin treatment (Figure 3i and j). Expression levels of succinyl-CoA-3-oxaloacid CoA transferase (SCOT), another enzyme critically involved in ketone metabolism, also remained unchanged (Figure 3i and j). Furthermore, empagliflozin did not alter expression level of branched-chain amino acid transaminase-2 (*Bcat2*), branched-chain alpha-ketoacid dehydrogenase complex, BCKDHA(Ser293)-phosphorylation and DBT, enzymes crucially involved in BCAA catabolism (Figure 3i, k and l).

We next performed untargeted metabolomic analyses from serum and cardiac tissue to further investigate substrate availability and utilization after 4.5 weeks of treatment on HFD. As expected, db/db mice presented with increased circulating and cardiac glucose concentrations relative to wild type controls, which were significantly reduced by empagliflozin treatment (Figure 4a and c). β-hydroxybutyrate and acetoacetate – the most abundant ketone bodies – were increased in the diabetic environment of

db/db mice and by trend reduced by empagliflozin treatment (Figure 4a and c). No difference in circulating or cardiac concentrations of lactate, BCAAs (Figure 4a-d) nor short-chain- and middle-chain fatty acids (data not shown) were found between groups. Empagliflozin however significantly increased carnitine coupling of long-chain fatty acids – required for mitochondrial entry and beta-oxidation – in serum, which was however not recapitulated in cardiac tissue (Figure 4e and g). No relevant differences in TCA cycle metabolites was found between groups, not indicating a relevant modulation of the final step of substrate oxidation by empagliflozin treatment (Figure 4f and h).

To better understand the empagliflozin-dependent improvement of the left ventricular diastolic function we assessed cardiac troponin I(Ser23/34)-phosphorylation, which we found to be increased in the diabetic environment of db/db mice while being significantly reduced by empagliflozin treatment. As troponin I-phosphorylation is known to reduce myofilament calcium sensitivity in response to adrenergic stimuli we next assessed activating phosphorylation of CaMKII(Thr286) which was reduced by empagliflozin treatment. Consistently, downstream CaMKII target RyR(Ser2808)-phosphorylation was similarly reduced by empagliflozin. This observation suggests empagliflozin-dependent improvement of diastolic function of db/db mice to be caused by reduced RyR-dependent spontaneous diastolic sarcoplasmic reticulum calcium leak.

4. Discussion

The present study shows a reduction in mortality after 4.5 weeks of treatment with the SGLT2 inhibitor empagliflozin in db/db mice on HFD which was accompanied by an improvement in diastolic left ventricular function [12]. In this model, empagliflozin reduced circulating and cardiac concentrations of glucose levels with potential relevance for the observed improvement of left ventricular diastolic function. Unexpectedly, empagliflozin did not affect circulating or cardiac metabolites of ketone bodies or BCAAs nor the expression of enzymes critically involved in their catabolism in this model. Empagliflozin however reduced cardiac CaMKII(Thr286)-activation with lower downstream RyR(Ser2808)-phosphorylation as a cause for spontaneous diastolic sarcoplasmic reticulum calcium leak which is a relevant mechanism for diastolic left ventricular dysfunction.

Diastolic dysfunction is characterized by slow or incomplete relaxation of the ventricles during diastole and is an important contributor to heart failure pathophysiology mainly driven by calcium mishandling and interstitial fibrosis [13]. During systole, intracellular Ca^{2+} is released from the sarcoplasmic reticulum into the cytoplasm through type-2 ryanodine receptor/Ca^{2+} release channels. In heart failure, chronically elevated circulating catecholamine levels cause pathological remodeling of type-2 ryanodine receptor/Ca^{2+} release channels resulting in diastolic sarcoplasmic reticulum Ca^{2+} leak and decreased myocardial contractility [14].

In recent CV outcome trials, SGLT2 inhibitors like empagliflozin, canagliflozin, and dapagliflozin have been shown to reduce heart failure hospitalization in patients with type 2 diabetes and/or preexisting heart failure [1-3]. The exact underlying mechanisms for this finding remain incompletely understood but hemodynamic effects, a reduction of total body sodium content as well as direct effects on cardiac energy metabolism – among other modes of action – have been discussed extensively [5-8].

In this model we found SGLT2 inhibition to improve diastolic function of db/db mice on HFD. This is consistent with results of others studies in rodent and human [15, 16]. Blood glucose lowering by SGLT2 inhibition leads to a fasting response of the organism indicated by an elevation of glucagon levels and the formation of ketone bodies which has been reported in a variety of studies [17]. A consequential switch in substrate utilization from glucose to other substrates including lactate, fatty acids, BCAAs and ketone bodies have been suggested to provide additional energy for the functionally impaired cardiac muscle. Heart failure favors the uptake of glucose and free fatty acids by cardiomyocytes. Insufficient capacity to shuttle these substrates to the mitochondria for oxidation causes cytosolic accumulation with disturbance of cellular hemostasis termed gluco- and lipotoxicity [18]. Similar mechanisms have been identified to be relevant for diabetes-induced cardiomyopathy together with cardiac insulin resistance and impaired metabolic flexibility [19, 20]. As an alternative substrate ketone bodies have been suggested to overcome these limitations and directly fuel the TCA cycle in an insulin-independent manner [4]. This concept is intriguing since cardiac ketone body metabolism was recently identified as an important mechanism to provide alternative energy supply for the failing heart [11].

Given an elevation of circulating ketone bodies upon SGLT2 inhibitor treatment, it has been hypothesized that an increase in cardiac ketone utilization may contribute to the beneficial effects seen in the different CV-outcome trials with this class of drugs [21, 22].

Unexpectedly, empagliflozin did not increase but rather reduced ketone body abundance in serum and cardiac tissue of db/db mice on HFD in our model. As ketone body formation is part of the stress response of the organism, this might be indicative for increased metabolic stress of the control group under more severe diabetic conditions [23]. This interpretation is supported by reduced hepatic inflammation and mortality of empagliflozin treated db/db mice in our experiment. Unaltered cardiac expression of relevant ketone catabolizing enzymes does not suggest the relevance of ketone body metabolism for improvement of left ventricular diastolic function in our model. In contrast, empagliflozin reduced circulating and cardiac glucose concentrations, which might be indicative for increased metabolic flexibility as a possible cause for improved diastolic function. This was paralleled by increased cardiac AKT(Thr308)-phosphorylation as a possible indicator of improved insulin signaling in our model. Similarly, others have found empagliflozin to significantly increase cardiac AKT-phosphorylation in ob/ob mice [24]. In contrast, SGLT2 inhibition did not affect cardiac AKT-signaling in ischemic myocardium following acute myocardial infarction, which most likely reflects differential experimental conditions [25].

Reduced glucotoxicity might also explain the decreased inflammatory response found in liver tissue, which warrants further investigations [18]. Interestingly empagliflozin also increased carnitine coupling of circulating long-chain fatty acids. As carnitine coupling is a necessary prerequisite for mitochondrial entry and beta-oxidation of fatty acids, this suggests SGLT2 inhibition to increase fatty acid catabolism in our model [26, 27]. The same signature was however not found in cardiac tissue. Additional investigations including flux analysis will be required to understand the consequences of SGLT2 inhibition for cardiac fatty acid oxidation. Others have reported cardiac fatty acid oxidation to be increased by SGLT2 inhibition in a non-diabetic pig model of ischemic cardiomyopathy, while unaltered fatty acid flux was reported in the hearts of empagliflozin treated db/db mice under *ex vivo* working heart conditions. Also, we did not find indications for altered lactate and BCAA metabolism

by SGLT2 inhibition in this model, which has been reported to be increased by other investigators [28].

Our study has certain strengths and limitations. Our mouse model of db/db mice on HFD is a model of severe diabetes with extensive metabolic disarrangements beyond diabetes alone. Thus, neither metabolic nor cardiac effects can be extrapolated to other diabetes models or the human situation. We only performed snapshot metabolomic analysis but did not detect energy substrate flux. This was combined with expression analysis of enzymes previously been shown to be a hallmark of altered ketone and BCAA metabolism in heart failure [10, 11, 29]. However, the lack of an effect on the expression levels of enzymes involved in ketone and BCAA metabolism seen in our study may be related to our model of severe diabetes and may not apply to other models of the human situation. Importantly, our study suggests SGLT2 inhibition to augment myocardial calcium handling as a mechanism of improved diastolic function. This observation requires confirmation and further mechanistic elaboration. As an additional limitation cardiac contractility was only performed by pressure catheter and not by echocardiographic analysis. Finally, the present study cannot explain the dramatic reduction in mortality by empagliflozin in our db/db mice. Potential mechanisms may include effects on calcium metabolism or sodium content with subsequent relevance for cardiac arrhythmias [5, 30, 31]. Diabetes is considered a state of sodium overload and increased intracellular sodium in the myocardium may increase the risk of arrhythmias and impair myocardial function [32]. Interestingly, experimental data in an animal model of heart failure showed an increase in myocardial intracellular sodium and in this model the blockade of the mitochondrial Na^+/Ca^{2+} exchange prolonged survival of these animals and significantly decreased arrhythmias in the heart [32]. SGLT2 inhibition leads to an early and transient increase in urinary sodium excretion with a subsequent reduction in total body and intracellular sodium content which may in the heart reduce the risk for arrhythmias [5]. Still, future work is warranted to further elaborate the mechanisms contributing to the mortality benefit seen in patients in recent CVOTs as well as in our murine model of diabetes.

5. Conclusion

In conclusion, our study in a murine model of severe diabetes suggest a beneficial effect of the SGLT2 inhibitor empagliflozin on mortality and diastolic function which might be mediated by improved cardiomyocyte Ca^{2+} handling.

Source of Funding

The project was supported by a grant from Boehringer Ingelheim to M.L., the German Research Foundation (DFG) SFB/Transregio 219 (SFB-TRR) “Mechanisms of Cardiovascular Complications in Chronic Kidney Disease” to K.S., N.M. and M.L. (DFG, TTR 219, C-07, M-03, M-05), INTERREG EURLIPIDS to N.M. and M.L., a grant of the CORONA foundation to N.M., M.L. and K.S. and the „START-program“ of the Medicine Faculty of the RWTH Aachen to J.M. and M.L.. This study was co-financed by the German Research Foundation (DFG: SFB/TRR57 and SFB/TRR219, BO3755/3-1 and BO3755/6-1), the German Ministry of Education and Research (BMBF: STOP-FSGS-01GM1518A) to P.B..

Disclosures

N.M. has received support for clinical trial leadership from Boehringer Ingelheim, N.M. has served as a consultant to Amgen, Bayer, Boehringer Ingelheim, Sanofi-Aventis, MSD, BMS, AstraZeneca, NovoNordisk and and has received grant support from Boehringer Ingelheim and MSD. In addition, N.M. has served as speaker for Amgen, Bayer, Boehringer Ingelheim, Sanofi-Aventis, MSD, BMS, AstraZeneca, Lilly, NovoNordisk. N.M. declines all personal compensation from pharma or device companies. M.L. has received grant support for experimental and clinical studies from Boehringer Ingelheim and MSD; has served as a consultant to Boehringer Ingelheim, Sanofi-Aventis, MSD, AstraZeneca, Lilly, NovoNordisk, Amgen and Bayer. Has served as a speaker for Boehringer Ingelheim Sanofi-Aventis, MSD, AstraZeneca, Lilly, NovoNordisk and Bayer. S.V. has recieved speaker honoraria from Abbott, Amgen, AstraZeneca, Bayer, Boheringer Ingelheim, Eli Lilly, Janssen, Merck, NovoNordisk, and Sanofi; and received research grant support from Amgen, AstraZeneca, Boheringer Ingelheim, and Eli Lilly. G.D.L.: shareholder in Metabolic Modulators Research Ltd, received grant support from Servier, Boehringer Ingelheim, Sanofi, REMED Biopharmaceuticals. K.S. has received grant support for

experimental studies from Boehringer Ingelheim and has served as speaker for Boehringer Ingelheim, Amgen, MSD, Omniamed and NovoNordisk. All other authors report no relevant disclosures.

Figure legends

Figure 1: Empagliflozin improves glucose metabolism and reduces mortality

Db/db mice (n=13 per group) and adequate db/db (wt) control mice (n=6 per group) were fed a HFD with or without empagliflozin. Empagliflozin increased urinary glucose excretion (a) and decreased fasting blood glucose (b) with no effect on body weight (c). Serum cholesterol was reduced by empagliflozin treatment while triglycerides were not changed (d). Liver weight was significantly reduced by empagliflozin treatment (e), with no change in hepatic lipid or β-hydroxybutyrate content (f). Hepatic mRNA expression (g and h) of db/db mice treated with or without empagliflozin in comparison to db/db (wt) control. Furthermore, empagliflozin led to a significant reduction of mortality (i) in diabetic db/db mice. Results are expressed as mean ± SEM. 1-way ANOVA; *p<0.05, **p<0.01, ***p<0.001 and ****p<0.0001.

Figure 2: Empagliflozin improves diastolic left ventricular function

Empagliflozin significantly improved left ventricular relaxation of db/db mice (a) while affecting left ventricular contractility only by trend (b). No differences in heart rate (c) between groups before and during dobutamine stress by final Millar catheter (db/db (wt): n=6, db/db: n=5 and db/db + Empa: n=11). No difference of heart weight (d), serum BNP levels (e), cardiac ANP protein nor mRNA expression (f-h) nor histological cardiac fibrosis (i and j) and left ventricular septal sickness (k) as well as for cardiomyocyte diameter and area (i, l and m) under empagliflozin treatment. Scale bar, 25 µm. Results are expressed as mean ± SEM. 1-way ANOVA; **p<0.01.

Figure 3: Empagliflozin treatment did not affect mitochondrial biogenesis nor expression of enzymes relevant for ketone and BCAA metabolism

Western blot analysis of cardiac glucose and energy metabolism (a-d) and cardiac mRNA expression of mitochondrial marker (mitochondrial transcription factors (f), genes for mitochondrial fusion and fission (g and h)) from db/db mice treated with or without empagliflozin in comparison to db/db (wt) control mice. Protein analysis of

cardiac tissue for ketone (i and j) and BCAA metabolism by western blot and PCR (i, k and l) (WB: n=5 per group; RNA: db/db (wt): n=3, db/db: n=4-5 and db/db + Empa: n=5-6). Results are expressed as mean ± SEM. 1-way ANOVA; *p<0.05 and ****p<0.0001.

Figure 4: Empagliflozin treatment increases carnitine coupling of long-chain fatty acids

Metabolome analysis showed an increase of circulating (a) and cardiac (d) glucose levels in db/db mice which were significantly decreased by empagliflozin treatment. Beta-hydroxybutyrate was also increased in db/db mice and decreased by trend under empagliflozin treatment (serum (b) and cardiac tissue (e)). No difference in circulating (c) and cardiac (f) concentrations of BCAA was found between groups. Empagliflozin significantly increased circulating carnitine coupling of long-chain fatty acids (g) while not affecting cardiac level (i). No change in TCA cycle metabolites (serum (h) and cardiac tissue (j)) (nd=not detectable). Results are expressed as mean ± SEM. 1-way ANOVA; *p<0.05, **p<0.01 and ***p<0.001.

Figure 5: Empagliflozin treatment reduces RyR-dependent spontaneous diastolic sarcoplasmic reticulum calcium leak

Western blot analysis of cardiac troponin I phosphorylation, CaMKII(Thr286)-phosphorylation as well as downstream RyR(Ser2808)-phosphorylation from db/db mice treated with or without empagliflozin in comparison to db/db (wt) control mice (n=5 per group). Results are expressed as mean ± SEM. 1-way ANOVA; *p<0.05 and **p<0.01.

References

1. Zinman, B., et al., *Empagliflozin, Cardiovascular Outcomes, and Mortality in Type 2 Diabetes.* N Engl J Med, 2015. **373**(22): p. 2117-28.
2. Neal, B., et al., *Canagliflozin and Cardiovascular and Renal Events in Type 2 Diabetes.* N Engl J Med, 2017. **377**(7): p. 644-657.
3. Wiviott, S.D., I. Raz, and M.S. Sabatine, *Dapagliflozin and Cardiovascular Outcomes in Type 2 Diabetes. Reply.* N Engl J Med, 2019. **380**(19): p. 1881-1882.
4. Verma, S., et al., *Empagliflozin Increases Cardiac Energy Production in Diabetes: Novel Translational Insights Into the Heart Failure Benefits of SGLT2 Inhibitors.* JACC Basic Transl Sci, 2018. **3**(5): p. 575-587.

5. Marx, N. and D.K. McGuire, *Sodium-glucose cotransporter-2 inhibition for the reduction of cardiovascular events in high-risk patients with diabetes mellitus.* Eur Heart J, 2016. **37**(42): p. 3192-3200.
6. Packer, M. and D.W. Kitzman, *Obesity-Related Heart Failure With a Preserved Ejection Fraction: The Mechanistic Rationale for Combining Inhibitors of Aldosterone, Neprilysin, and Sodium-Glucose Cotransporter-2.* JACC Heart Fail, 2018. **6**(8): p. 633-639.
7. Lytvyn, Y., et al., *Sodium Glucose Cotransporter-2 Inhibition in Heart Failure: Potential Mechanisms, Clinical Applications, and Summary of Clinical Trials.* Circulation, 2017. **136**(17): p. 1643-1658.
8. Ferrannini, E., M. Mark, and E. Mayoux, *CV Protection in the EMPA-REG OUTCOME Trial: A "Thrifty Substrate" Hypothesis.* Diabetes Care, 2016. **39**(7): p. 1108-14.
9. Kappel, B.A., et al., *Effect of Empagliflozin on the Metabolic Signature of Patients With Type 2 Diabetes Mellitus and Cardiovascular Disease.* Circulation, 2017. **136**(10): p. 969-972.
10. Aubert, G., et al., *The Failing Heart Relies on Ketone Bodies as a Fuel.* Circulation, 2016. **133**(8): p. 698-705.
11. Bedi, K.C., Jr., et al., *Evidence for Intramyocardial Disruption of Lipid Metabolism and Increased Myocardial Ketone Utilization in Advanced Human Heart Failure.* Circulation, 2016. **133**(8): p. 706-16.
12. Moellmann, J., et al., *Glucagon-Like Peptide 1 and Its Cleavage Products Are Renoprotective in Murine Diabetic Nephropathy.* Diabetes, 2018. **67**(11): p. 2410-2419.
13. Asp, M.L., et al., *Calcium mishandling in diastolic dysfunction: mechanisms and potential therapies.* Biochim Biophys Acta, 2013. **1833**(4): p. 895-900.
14. Kushnir, A., et al., *Ryanodine Receptor Calcium Leak in Circulating B-Lymphocytes as a Biomarker in Heart Failure.* Circulation, 2018. **138**(11): p. 1144-1154.
15. Habibi, J., et al., *Sodium glucose transporter 2 (SGLT2) inhibition with empagliflozin improves cardiac diastolic function in a female rodent model of diabetes.* Cardiovasc Diabetol, 2017. **16**(1): p. 9.
16. Pabel, S., et al., *Empagliflozin directly improves diastolic function in human heart failure.* Eur J Heart Fail, 2018. **20**(12): p. 1690-1700.
17. Al Jobori, H., et al., *Determinants of the increase in ketone concentration during SGLT2 inhibition in NGT, IFG and T2DM patients.* Diabetes Obes Metab, 2017. **19**(6): p. 809-813.
18. Maack, C., et al., *Heart failure and diabetes: metabolic alterations and therapeutic interventions: a state-of-the-art review from the Translational Research Committee of the Heart Failure Association-European Society of Cardiology.* Eur Heart J, 2018. **39**(48): p. 4243-4254.
19. Jia, G., A. Whaley-Connell, and J.R. Sowers, *Diabetic cardiomyopathy: a hyperglycaemia- and insulin-resistance-induced heart disease.* Diabetologia, 2018. **61**(1): p. 21-28.
20. Ferrannini, E., et al., *Shift to Fatty Substrate Utilization in Response to Sodium-Glucose Cotransporter 2 Inhibition in Subjects Without Diabetes and Patients With Type 2 Diabetes.* Diabetes, 2016. **65**(5): p. 1190-5.
21. Ferrannini, E., M. Mark, and E. Mayoux, *Response to Comment on Ferrannini et al. Diabetes Care 2016;39:1108-1114. Comment on Mudaliar et al. Diabetes Care 2016;39:1115-1122.* Diabetes Care, 2016. **39**(11): p. e196-e197.
22. Vallon, V. and S.C. Thomson, *Targeting renal glucose reabsorption to treat hyperglycaemia: the pleiotropic effects of SGLT2 inhibition.* Diabetologia, 2017. **60**(2): p. 215-225.
23. Puchalska, P. and P.A. Crawford, *Multi-dimensional Roles of Ketone Bodies in Fuel Metabolism, Signaling, and Therapeutics.* Cell Metab, 2017. **25**(2): p. 262-284.
24. Hammoudi, N., et al., *Empagliflozin Improves Left Ventricular Diastolic Dysfunction in a Genetic Model of Type 2 Diabetes.* Cardiovasc Drugs Ther, 2017. **31**(3): p. 233-246.
25. Andreadou, I., et al., *Empagliflozin Limits Myocardial Infarction in Vivo and Cell Death in Vitro: Role of STAT3, Mitochondria, and Redox Aspects.* Front Physiol, 2017. **8**: p. 1077.

26. Longo, N., M. Frigeni, and M. Pasquali, *Carnitine transport and fatty acid oxidation.* Biochim Biophys Acta, 2016. **1863**(10): p. 2422-35.
27. Hynes, M.J., et al., *Role of carnitine acetyltransferases in acetyl coenzyme A metabolism in Aspergillus nidulans.* Eukaryot Cell, 2011. **10**(4): p. 547-55.
28. Santos-Gallego, C.G., et al., *Empagliflozin Ameliorates Adverse Left Ventricular Remodeling in Nondiabetic Heart Failure by Enhancing Myocardial Energetics.* J Am Coll Cardiol, 2019. **73**(15): p. 1931-1944.
29. Sun, H., et al., *Catabolic Defect of Branched-Chain Amino Acids Promotes Heart Failure.* Circulation, 2016. **133**(21): p. 2038-49.
30. Bertero, E., et al., *Cardiac effects of SGLT2 inhibitors: the sodium hypothesis.* Cardiovasc Res, 2018. **114**(1): p. 12-18.
31. Packer, M., et al., *Effects of Sodium-Glucose Cotransporter 2 Inhibitors for the Treatment of Patients With Heart Failure: Proposal of a Novel Mechanism of Action.* JAMA Cardiol, 2017. **2**(9): p. 1025-1029.
32. Liu, T., et al., *Inhibiting mitochondrial Na+/Ca2+ exchange prevents sudden death in a Guinea pig model of heart failure.* Circ Res, 2014. **115**(1): p. 44-54.

Declaration of interests

☐ The authors declare that they have no known competing financial interests or personal relationships that could have appeared to influence the work reported in this paper.

☒The authors declare the following financial interests/personal relationships which may be considered as potential competing interests:

N.M. has received support for clinical trial leadership from Boehringer Ingelheim, **N.M.** has served as a consultant to Amgen, Bayer, Boehringer Ingelheim, Sanofi-Aventis, MSD, BMS, AstraZeneca, NovoNordisk and and has received grant support from Boehringer Ingelheim and MSD. In addition, **N.M.** has served as speaker for Amgen, Bayer, Boehringer Ingelheim, Sanofi-Aventis, MSD, BMS, AstraZeneca, Lilly, NovoNordisk. **N.M.** declines all personal compensation from pharma or device companies. **M.L.** has received grant support for experimental and clinical studies from Boehringer Ingelheim and MSD; has served as a consultant to Boehringer Ingelheim, Sanofi-Aventis, MSD, AstraZeneca, Lilly, NovoNordisk, Amgen and Bayer. Has served as a speaker for Boehringer Ingelheim Sanofi-Aventis, MSD, AstraZeneca, Lilly, NovoNordisk and Bayer. **S.V.** has recieved speaker honoraria from Abbott, Amgen, AstraZeneca, Bayer, Boheringer Ingelheim, Eli Lilly, Janssen, Merck, NovoNordisk, and Sanofi; and received research grant support from Amgen, AstraZeneca, Boheringer Ingelheim, and Eli Lilly. **G.D.L.:** shareholder in Metabolic Modulators Research Ltd, received grant support from Servier, Boehringer Ingelheim, Sanofi, REMED Biopharmaceuticals. **K.S.** has received grant support for experimental studies from Boehringer Ingelheim and has served as speaker for Boehringer Ingelheim, Amgen, MSD, Omniamed and NovoNordisk. All other authors report no relevant disclosures.

HIGHLIGHTS

- This study investigates the effects of empagliflozin dependent SGLT2 inhibition on glucose metabolism, cardiac function and cardiac substrate utilization in severely diabetic db/db mice on high fat diet.
- Empagliflozin improved glucose metabolism, reduced mortality and ameliorated left ventricular diastolic function of db/db mice.
- Not effect of empagliflozin was noted on systemic levels of ketone bodies or cardiac expression of enzymes relevant for ketone body or branched chain amino acid catabolism.
- We conclude in a murine model of severe diabetes suggest a beneficial effect of the SGLT2 inhibitor empagliflozin on mortality and diastolic function which might be mediated by improved cardiomyocyte Ca^{2+} handling.

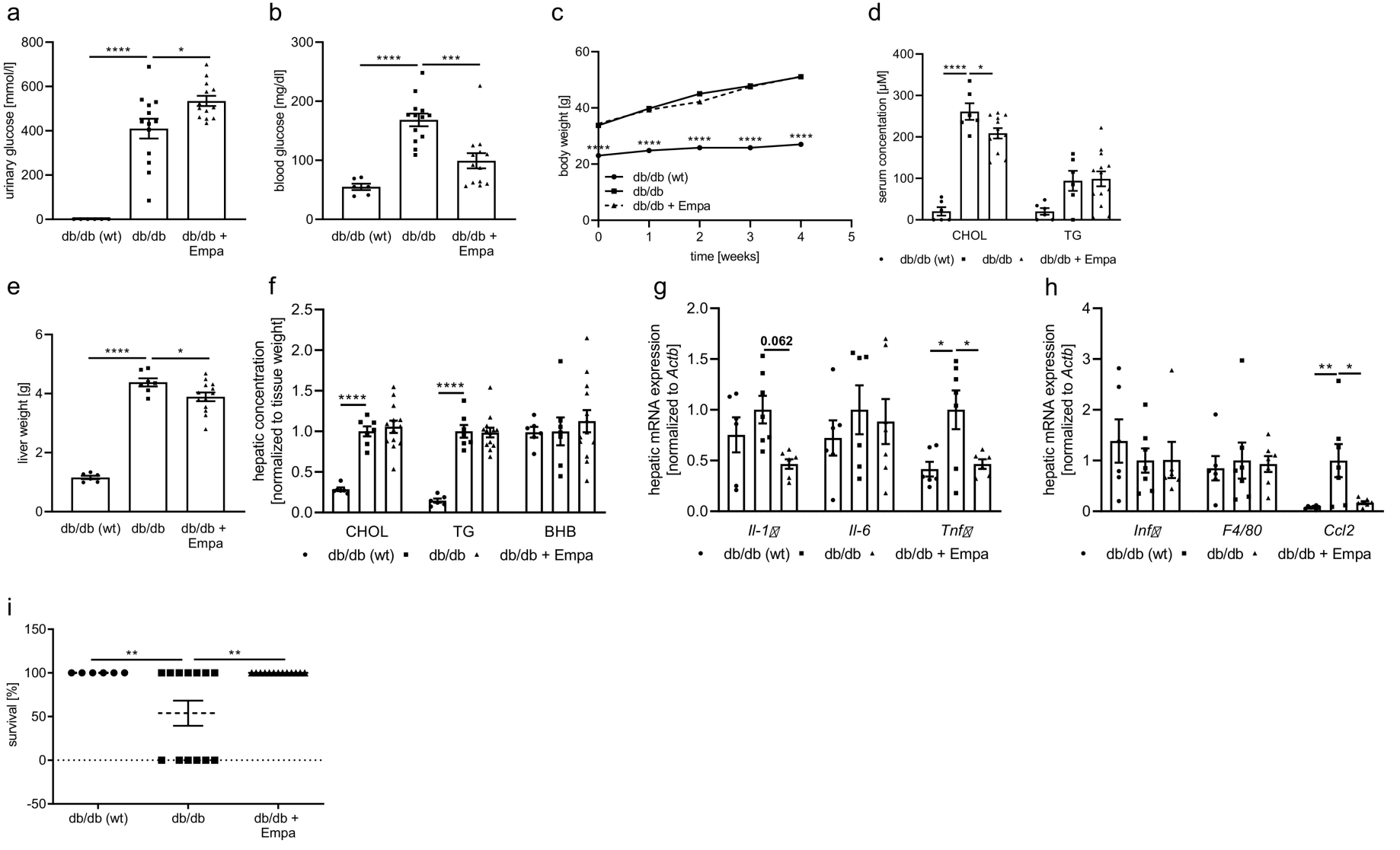
a
urinary glucose [mmol/l]
db/db (wt)
db/db
db/db + Empa
b
blood glucose [mg/dl]
c
body weight [g]
time [weeks]
db/db (wt)
db/db
db/db + Empa
d
serum concentation [µM]
CHOL
TG
e
liver weight [g]
f
hepatic concentration [normalized to tissue weight]
CHOL
TG
BHB
g
hepatic mRNA expression [normalized to Actb]
0.062
Il-1β
Il-6
Tnfα
h
Infα
F4/80
Ccl2
i
survival [%]

Figure 1

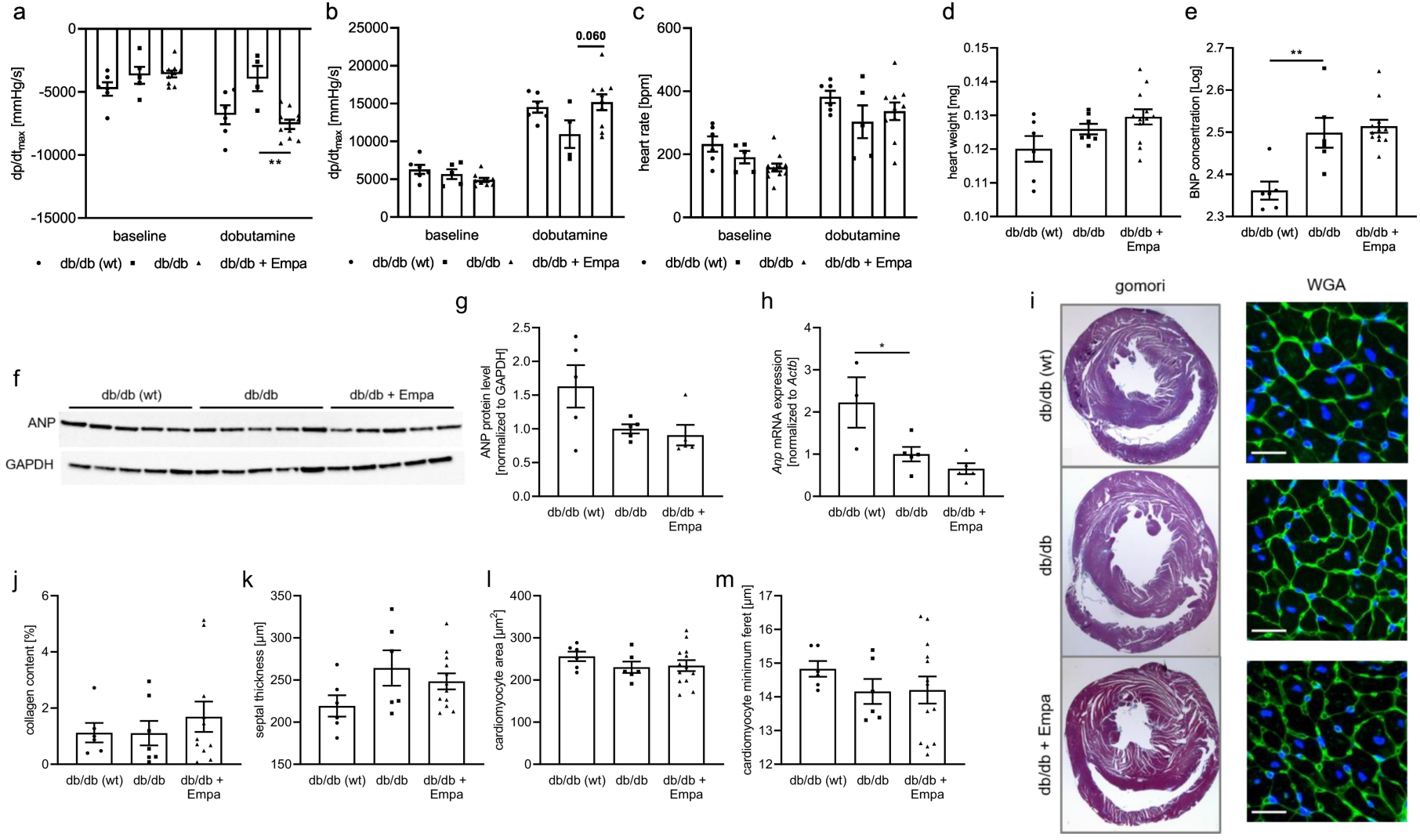
a
b
c
d
e
f
g
h
i
j
k
l
m
dp/dtmax [mmHg/s]
baseline
dobutamine
db/db (wt)
db/db
db/db + Empa
0.060
**
heart rate [bpm]
heart weight [mg]
BNP concentration [Log]
ANP
GAPDH
ANP protein level [normalized to GAPDH]
Anp mRNA expression [normalized to Actb]
*
gomori
WGA
collagen content [%]
septal thickness [µm]
cardiomyocyte area [µm²]
cardiomyocyte minimum feret [µm]

Figure 2

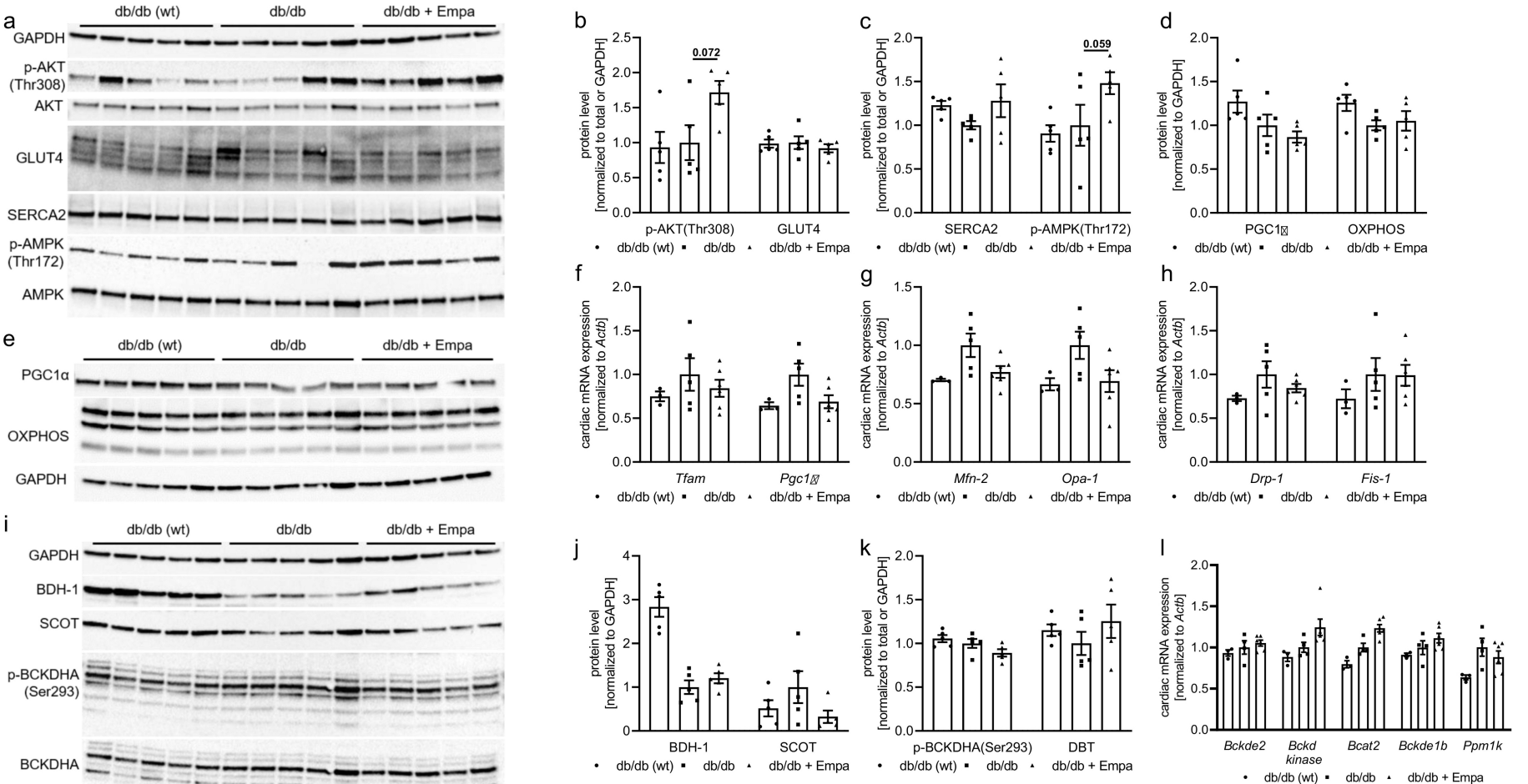
a
db/db (wt)
db/db
db/db + Empa
GAPDH
p-AKT (Thr308)
AKT
GLUT4
SERCA2
p-AMPK (Thr172)
AMPK
b
protein level [normalized to total or GAPDH]
0.072
p-AKT(Thr308)
GLUT4
c
0.059
SERCA2
p-AMPK(Thr172)
d
protein level [normalized to GAPDH]
PGC1α
OXPHOS
e
PGC1α
OXPHOS
GAPDH
f
cardiac mRNA expression [normalized to Actb]
Tfam
Pgc1α
g
Mfn-2
Opa-1
h
Drp-1
Fis-1
i
BDH-1
SCOT
p-BCKDHA (Ser293)
BCKDHA
DBT
j
k
l
Bckde2
Bckd kinase
Bcat2
Bckde1b
Ppm1k

Figure 3

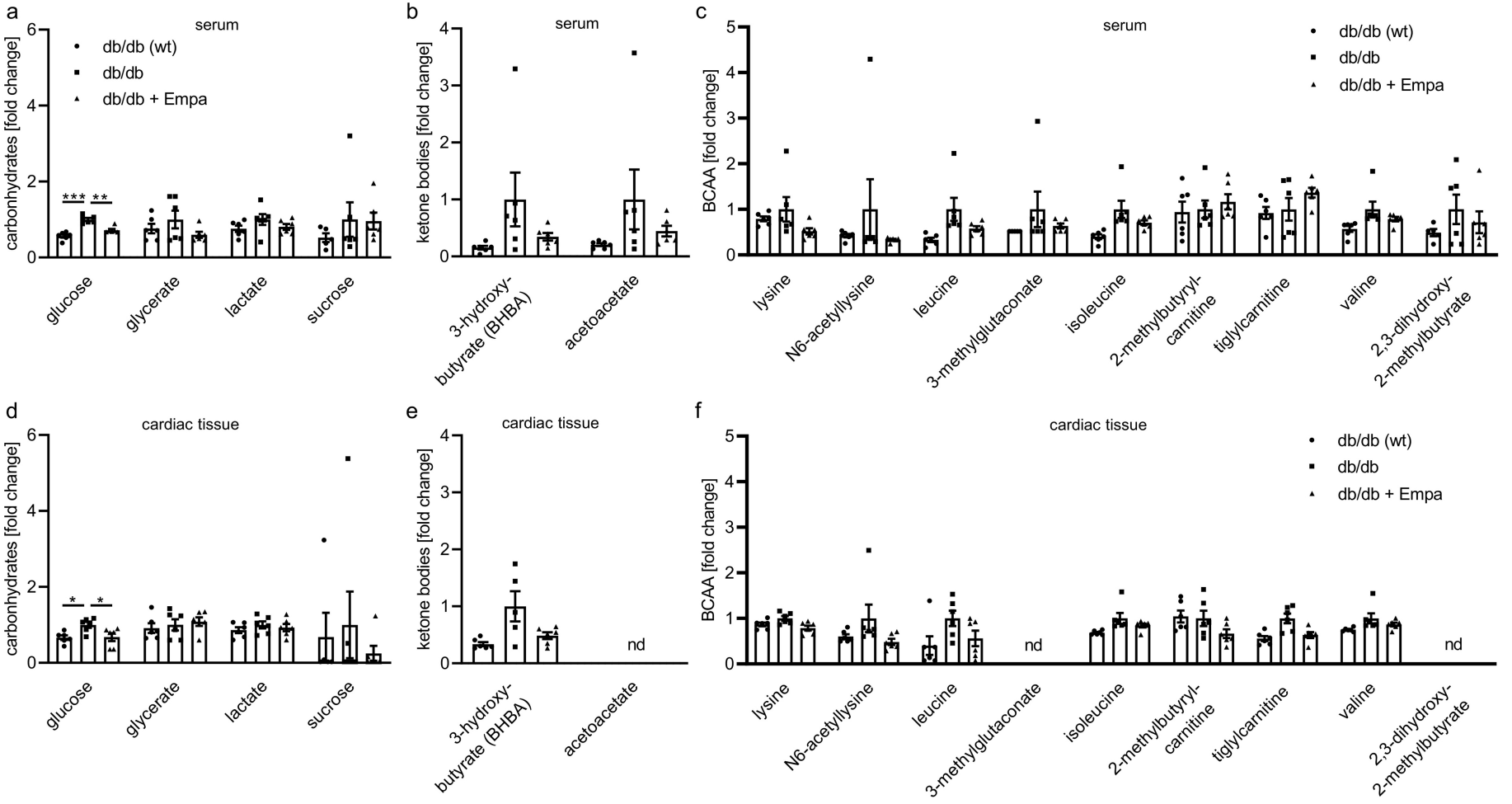
a
serum
db/db (wt)
db/db
db/db + Empa
carbonhydrates [fold change]
***
**
glucose
glycerate
lactate
sucrose
b
serum
ketone bodies [fold change]
3-hydroxy-butyrate (BHBA)
acetoacetate
c
serum
BCAA [fold change]
lysine
N6-acetyllysine
leucine
3-methylglutaconate
isoleucine
2-methylbutyryl-carnitine
tiglylcarnitine
valine
2,3-dihydroxy-2-methylbutyrate
d
cardiac tissue
carbonhydrates [fold change]
*
*
e
cardiac tissue
ketone bodies [fold change]
nd
f
cardiac tissue
BCAA [fold change]
nd
nd

Figure 4af

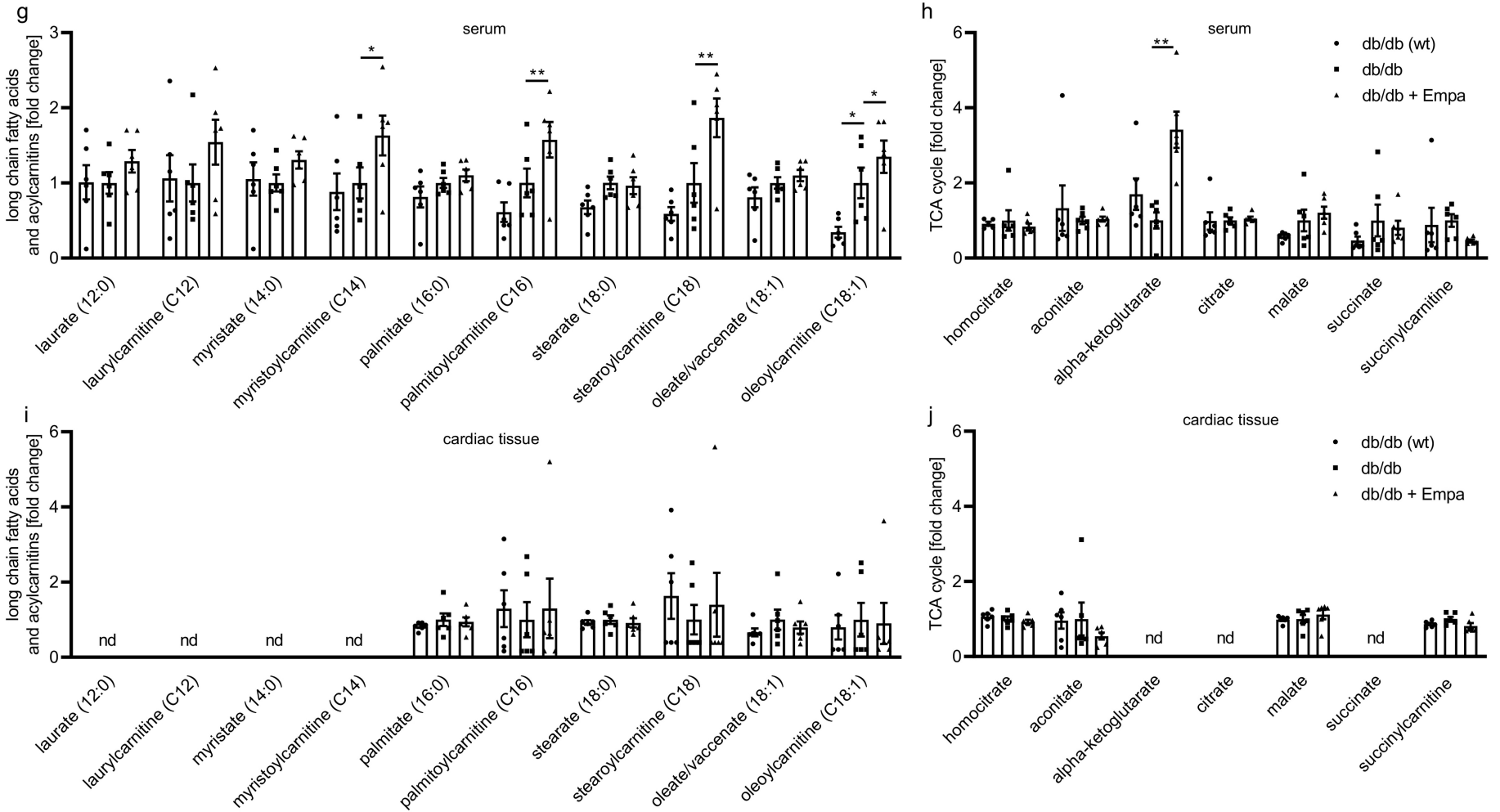
g
serum
long chain fatty acids and acylcarnitins [fold change]
laurate (12:0)
laurylcarnitine (C12)
myristate (14:0)
myristoylcarnitine (C14)
palmitate (16:0)
palmitoylcarnitine (C16)
stearate (18:0)
stearoylcarnitine (C18)
oleate/vaccenate (18:1)
oleoylcarnitine (C18:1)
h
serum
TCA cycle [fold change]
db/db (wt)
db/db
db/db + Empa
homocitrate
aconitate
alpha-ketoglutarate
citrate
malate
succinate
succinylcarnitine
i
cardiac tissue
nd
j
cardiac tissue

Figure 4gj

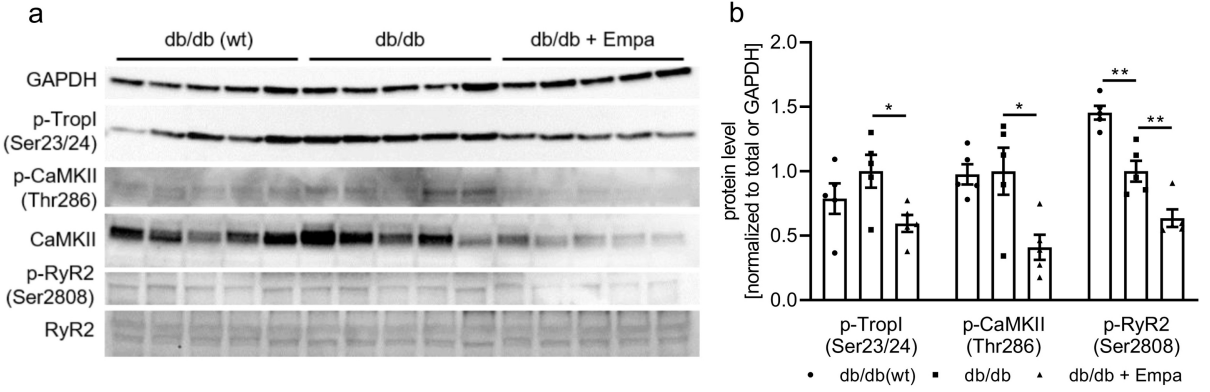
a
db/db (wt)
db/db
db/db + Empa
GAPDH
p-TropI (Ser23/24)
p-CaMKII (Thr286)
CaMKII
p-RyR2 (Ser2808)
RyR2
b
protein level [normalized to total or GAPDH]
2.0
1.5
1.0
0.5
0.0
*
*
**
**
p-TropI (Ser23/24)
p-CaMKII (Thr286)
p-RyR2 (Ser2808)
db/db(wt)
db/db
db/db + Empa

Figure 5